

Approximate Solution of a Fractional-Order Ebola Virus Disease Model with Contact Tracing and Quarantine

Akinyemi Samuel Tosin^{1*}, Oyelowo Yemisi², Ibrahim Mohammed Olarenwaju³, Adamu Bala⁴

¹Department of Mathematics, Tai Solarin College of Education, Ogun State, Nigeria.

²Department of Mathematics, Waziri Umaru Federal Polytechnic, Binrin Kebbi, Kebbi State, Nigeria.

³Department of Mathematics, University of Ilorin, Nigeria.

⁴Department of Basic Sciences, Federal Polytechnic, Auchu Edo State, Nigeria.

* Corresponding author: Sammysalt047@gmail.com

Received: 23 September 2022

Accepted: 17 January 2023

ABSTRACT

An elegant approximation of the fractional-order epidemic model's for Ebola Virus Disease (EVD) transmission combined with contact tracing and quarantine is presented in this study. The EVD model is governed by a system of nonlinear ordinary differential equations of fractional order described in Caputo sense. The Adams-Bashforth-Moulton algorithm is applied to simulate the model and compared with Runge-Kutta method in the case of integer-order derivatives to validate its efficiency.

Keywords: Adams-Bashforth-Moulton Method, Caputo Derivatives, Ebola Virus Disease Model, Fractional Differential Equation

1 INTRODUCTION

Recently, the use of fractional calculus has continued to gain wide acceptance due to its vast applications to successfully describe various phenomena in science and engineering. The idea of fractional calculus was first mentioned in early 17th century by Leibniz [1]. Fractional calculus deals with the theory of derivatives and integrals of non-integer order [2] specifically, it encompasses both classical and non-integer order calculus. [3]. To be specific, as fractional calculus is found invaluable in various field, fractional differential equations have been implemented in control systems, viscoelasticity, electromagnetic waves, blood flow phenomena, polymer rheology, fitting of experimental data, magnetohydrodynamic flow [1,4,5] and particularly in mathematical biology [6-7]. This is due to the advantage of fractional order differential equations over integer order differential equations [8], as the former is inherently related to real life phenomena with memory effect which exist mostly in biological systems [3].

Several fractional order models for Ebola existing in literature are found in [9-11]. Due to the absence of exact solutions for most nonlinear fractional differential equations, numerical and semi analytic methods are usually used [12]. The numerical methods include Generalized Euler Method (GEM) [12], the predictor corrector of Adams-Bashforth-Moulton [1,13,14], Atanakovic and Stankovic Method [7], etc, while Laplace Adomian Decomposition Method (LADM), Homotopy Analysis Method

(HAM), Homotopy Perturbation Method (HPM), Variational Iteration Method (VIM), Differential Transform Method (DTM), Multi Step Differential Transform Method (MSDTM) [15] are semi-analytic techniques.

The purpose of this paper is to provide an approximate solution to a fractional-order Ebola epidemic model using Fractional Adams-Bashforth-Moulton method. The rest of the paper is organized as follows. Basic definition and model formulation is presented in section 2. Basic concept and application of FABM method is discussed in section 3. Section 4 gives numerical simulation and discussion of results while section 5 concludes the paper.

2 BASIC DEFINITION AND MODEL FORMULATION

The formulation of the fractional order EVD model with contact tracing and quarantine, as well as some fundamental definitions in fractional calculus, are presented in this section.

Definition 2.1. Riemann-Liouville fractional integration of order q is defined as:

$$J^q f(x) = \frac{1}{\Gamma(q)} \int_0^x (x-t)^{q-1} f(t) dt, \quad q > 0, \quad x > 0$$

$$J^0 f(x) = f(x)$$

Definition 2.2. Caputo and Riemann-Liouville fractional derivatives of order q are defined respectively as follows:

$$D_*^q f(x) = J^{m-q} (D^m f(x))$$

$$D^q f(x) = D^m (J^{m-q} f(x))$$

where $m-1 < q \leq m$, $m \in \mathbb{N}$

To derive the fractional-order EVD model that explains the spread of EVD in a community, we first consider EVD model of integer order presented in [16] as:

$$\begin{aligned} \frac{dS}{dt} &= \Pi - \frac{\beta SI}{N} + \sigma Q + \phi T - (\mu + c_1)S \\ \frac{dQ}{dt} &= \varepsilon + c_1 S - (\mu_1 + \phi + \sigma)Q \\ \frac{dI}{dt} &= \frac{\beta SI}{N} - (\mu + c_2 + \alpha + d_1)I \\ \frac{dT}{dt} &= (c_2 + \alpha)I + \phi Q - (\mu + \phi)T \end{aligned} \tag{1}$$

Subject to the following initial populations

$$S(0) = 4396521, \quad Q(0) = 74, \quad I(0) = 33, \quad T(0) = 9$$

where

$$N = S + Q + I + T.$$

Table 1: Description of State Variables

State Variables	Description of State Variables
$S(t)$	Population of Susceptible (those who healthy and prone to infection) Individuals at time t .
$Q(t)$	Population of Quarantined Individuals at time t .
$I(t)$	Population of Infected Individuals at time t .
$T(t)$	Population of Infected Individuals Receiving Treatment at time t .
$N(t)$	Total Population of Individuals within the Community at time t .

Table 2: Parameters Description and Hypothetical Values

Parameters	Symbols	Hypothetical Values
Disease transmission rate	β	0.160
Rate for detecting infected individuals due to contact tracing	c_2	0.07
Rate of detecting susceptible individuals who were exposed to Ebola Virus (EBOV) due to contact tracing	c_1	0.06
Rate of death caused by EVD	d_1	0.0301653
Immigration rate of susceptible populations	Π	422
Rate of losing immunity for those who recovered due to treatment	ϕ	0.047619
Immigration of those affected by Ebola	ε	0.0314862
Natural death rate for these classes - susceptible, infected and treatment	μ	0.00002465753

Death rate for those in isolation for the period of 2-21 days	μ_1	5×10^{-6}
Rate for detecting the infected individuals in isolation	φ	0.08333
Rate for locating infected individuals within the infected class	α	0.0608

Note: Source of Hypothetical Values [16]

Now considering historical effects, system (1) is written in terms of time dependent integrations as follows:

$$\begin{aligned}
 \frac{dS}{dt} &= \int_0^t g(t-p) \left[\Pi - \frac{\beta S(p)I(p)}{S(p)+Q(p)+I(p)+T(p)} + \sigma Q(p) + \phi T(p) - (\mu + c_1)S(p) \right] dp \\
 \frac{dQ}{dt} &= \int_0^t g(t-p) [\varepsilon + c_1 S(p) - (\mu_1 + \varphi + \sigma)Q(p)] dp \\
 \frac{dI}{dt} &= \int_0^t g(t-p) \left[\frac{\beta S(p)I(p)}{S(p)+Q(p)+I(p)+T(p)} - (\mu + c_2 + \alpha + d_1)I(p) \right] dp \\
 \frac{dT}{dt} &= \int_0^t g(t-p) [(c_2 + \alpha)I(p) + \varphi Q(p) - (\mu + \phi)T(p)] dp
 \end{aligned} \tag{2}$$

where $g(t-p)$ is a kernel with respect to time.

The power-law function is now chosen as the kernel for long-term historical effects, with the result that events that occurred in the distant past have a much smaller impact on the present than those that occurred in the near past. By definition, the power-law kernel is

$$g(t-p) = \frac{(t-p)^{q-2}}{\Gamma(q-1)} \tag{3}$$

Substituting (3) into (2) to have

$$\begin{aligned}
 \frac{dS}{dt} &= \frac{1}{\Gamma(q-1)} \int_0^t (t-p)^{q-2} \left[\Pi - \frac{\beta S(p)I(p)}{S(p)+Q(p)+I(p)+T(p)} + \sigma Q(p) + \phi T(p) - (\mu + c_1)S(p) \right] dp \\
 \frac{dQ}{dt} &= \frac{1}{\Gamma(q-1)} \int_0^t (t-p)^{q-2} [\varepsilon + c_1 S(p) - (\mu_1 + \varphi + \sigma)Q(p)] dp \\
 \frac{dI}{dt} &= \frac{1}{\Gamma(q-1)} \int_0^t (t-p)^{q-2} \left[\frac{\beta S(p)I(p)}{S(p)+Q(p)+I(p)+T(p)} - (\mu + c_2 + \alpha + d_1)I(p) \right] dp \\
 \frac{dT}{dt} &= \frac{1}{\Gamma(q-1)} \int_0^t (t-p)^{q-2} [(c_2 + \alpha)I(p) + \varphi Q(p) - (\mu + \phi)T(p)] dp
 \end{aligned} \tag{4}$$

By definition of fractional integral, system (4) becomes

$$\begin{aligned} \frac{dS}{dt} &= J^{q-1} \left[\Pi - \frac{\beta S(t)I(t)}{S(t)+Q(t)+I(t)+T(t)} + \sigma Q(t) + \phi T(t) - (\mu + c_1)S(t) \right] \\ \frac{dQ}{dt} &= J^{q-1} \left[\varepsilon + c_1 S(t) - (\mu_1 + \varphi + \sigma)Q(t) \right] \\ \frac{dI}{dt} &= J^{q-1} \left[\frac{\beta S(t)I(t)}{S(t)+Q(t)+I(t)+T(t)} - (\mu + c_2 + \alpha + d_1)I(t) \right] \\ \frac{dT}{dt} &= J^{q-1} \left[(c_2 + \alpha)I(t) + \varphi Q(t) - (\mu + \phi)T(t) \right]. \end{aligned} \tag{5}$$

By applying fractional derivative of order $q-1$ (that is J^{1-q}) on both sides of (5) followed with Definition 2.2, to obtain

$$\begin{aligned} D_*^q S(t) &= \Pi - \frac{\beta S(t)I(t)}{S(t)+Q(t)+I(t)+T(t)} + \sigma Q(t) + \phi T(t) - (\mu + c_1)S(t) \\ D_*^q Q(t) &= \varepsilon + c_1 S(t) - (\mu_1 + \varphi + \sigma)Q(t) \\ D_*^q I(t) &= \frac{\beta S(t)I(t)}{S(t)+Q(t)+I(t)+T(t)} - (\mu + c_2 + \alpha + d_1)I(t) \\ D_*^q T(t) &= (c_2 + \alpha)I(t) + \varphi Q(t) - (\mu + \phi)T(t). \end{aligned} \tag{6}$$

Thus, a fractional order mathematical model is suggested by the system to explain the spread of EVD in the presence of contact tracing and quarantine (6). Furthermore, in the absence of memory effect (when $q = 1$) [17], (6) becomes (1).

3 THE CONCEPT OF FRACTIONAL ADAMS - BASHFORTH - MOULTON METHOD

Considering the initial value problem

$$D_*^q y(t) = f(t, y(t)), \quad y(0) = y_0, \quad 0 < q \leq 1, \quad t \geq 0 \tag{7}$$

which is equivalent to the equation for the fractional integral

$$y(t) = y_0 + J^b f(t, y(t)). \tag{8}$$

Let $[0, T]$ be the interval of obtaining approximate solution of (8). The interval $[0, T]$ is subdivided into M subintervals of equal step size $h = \frac{T}{M}$ by using the nodes $t_j = jh$ and $y(t_j) = y_j$ for $j = 0, 1, \dots, M$.

The proposed method is a predictor corrector method in solving (8) such that an initial approximation $y_{P,K}$ called the predictor is evaluated first using the product rectangle rule as

$$y_{P,K} = y_0 + \frac{1}{\Gamma(q)} \sum_{j=0}^{K-1} b_{j,K} f(t_j, y_j) \quad (9)$$

which is then used to get the correct approximation y_K . The trapezoidal rule is used to evaluate

$$y_K = y_0 + \frac{1}{\Gamma(q)} \left(a_{K,K} f(t_K, y_{P,K}) + \sum_{j=0}^{K-1} a_{j,K} f(t_j, y_j) \right) \quad (10)$$

where the weight $a_{j,K}$ and $b_{j,K}$ are given by

$$a_{j,K} = \begin{cases} \frac{h^q}{q(q+1)} \left[(K-1)^{q+1} - K^q (k-1-q) \right], & j=0, \\ \frac{h^q}{q(q+1)} \left[(K+1-j)^{q+1} + (k-1-q)^{q+1} - 2(K-j)^{q+1} \right], & 1 \leq j \leq K-1, \\ \frac{h^q}{q(q+1)}, & j=K \end{cases} \quad (11)$$

and

$$b_{j,K} = \frac{h^q}{q} \left[(K-j)^q - (K-1-j)^q \right]. \quad (12)$$

4 APPLICATION OF FABM METHOD

The purpose of this section is to apply FABM method on (6), so we rewrite (6) as

$$\begin{aligned} D_*^q S(t) &= f_1(S, Q, I, T) \\ D_*^q Q(t) &= f_2(S, Q) \\ D_*^q I(t) &= f_3(S, Q, I, T) \\ D_*^q T(t) &= f_4(Q, I, T) \end{aligned} \quad (13)$$

such that

$$\begin{aligned}
 f_1(S, Q, I, T) &= \Pi - \frac{\beta S(t)I(t)}{S(t) + Q(t) + I(t) + T(t)} + \sigma Q(t) + \phi T(t) - (\mu + c_1)S(t) \\
 f_2(S, Q) &= \varepsilon + c_1 S(t) - (\mu_1 + \phi + \sigma)Q(t) \\
 f_3(S, Q, I, T) &= \frac{\beta S(t)I(t)}{S(t) + Q(t) + I(t) + T(t)} - (\mu + c_2 + \alpha + d_1)I(t) \\
 f_4(Q, I, T) &= (c_2 + \alpha)I(t) + \phi Q(t) - (\mu + \phi)T(t)
 \end{aligned}
 \tag{14}$$

Now, applying FABM method to (13) with the aid of (10) - (12) to have

$$\begin{aligned}
 S_K &= S_0 + \frac{h^q}{\Gamma(q)} \left[a_{K,K} f_1(S_{P,K}, Q_{P,K}, I_{P,K}, T_{P,K}) + \sum_{j=0}^{K-1} a_{j,K} f_1(t_j, S_j, Q_j, I_j, T_j) \right] \\
 Q_K &= Q_0 + \frac{h^q}{\Gamma(q)} \left[a_{K,K} f_2(S_{P,K}, Q_{P,K}) + \sum_{j=0}^{K-1} a_{j,K} f_2(S_j, Q_j) \right] \\
 I_K &= I_0 + \frac{h^q}{\Gamma(q)} \left[a_{K,K} f_3(S_{P,K}, Q_{P,K}, I_{P,K}, T_{P,K}) + \sum_{j=0}^{K-1} a_{j,K} f_3(S_j, Q_j, I_j, T_j) \right] \\
 T_K &= T_0 + \frac{h^q}{\Gamma(q)} \left[a_{K,K} f_4(Q_{P,K}, I_{P,K}, T_{P,K}) + \sum_{j=0}^{K-1} a_{j,K} f_4(Q_j, I_j, T_j) \right]
 \end{aligned}
 \tag{15}$$

5 NUMERICAL SIMULATIONS

The effectiveness of the FABM method is demonstrated graphically on time interval $[0,100]$ while using Maple 13 software with the value of parameters stated in Table 1 for different values of q . Figures 1-4 show the approximate solutions obtained using FABM method and when the inbuilt Maple 13 command for the fourth order Runge-Kutta method (RK4) is used for susceptible, quarantined, infectious and treated individuals respectively in the absence of memory/ historical effect (that is for $q = 1$). It can be seen that despite the time step h of RK4 is four times smaller to that of FABM method, both results are in excellent agreement with one another.

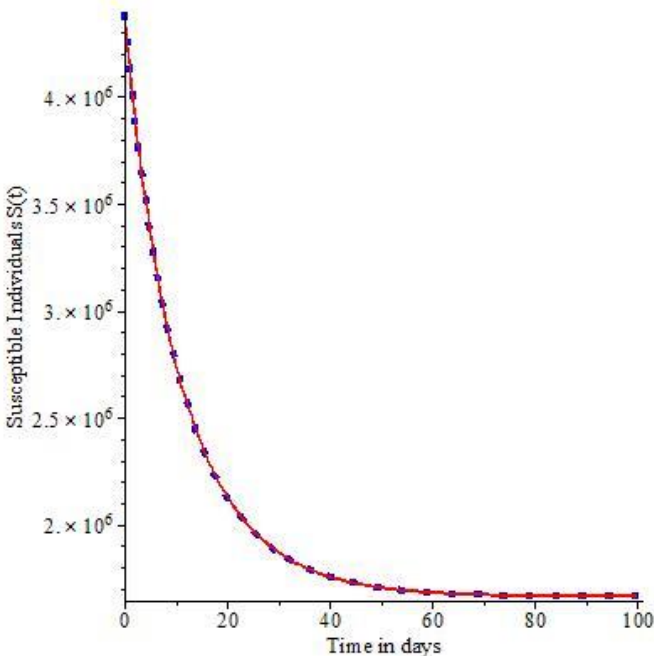


Figure 1: Comparison of FABM and RK4 for $S(t)$

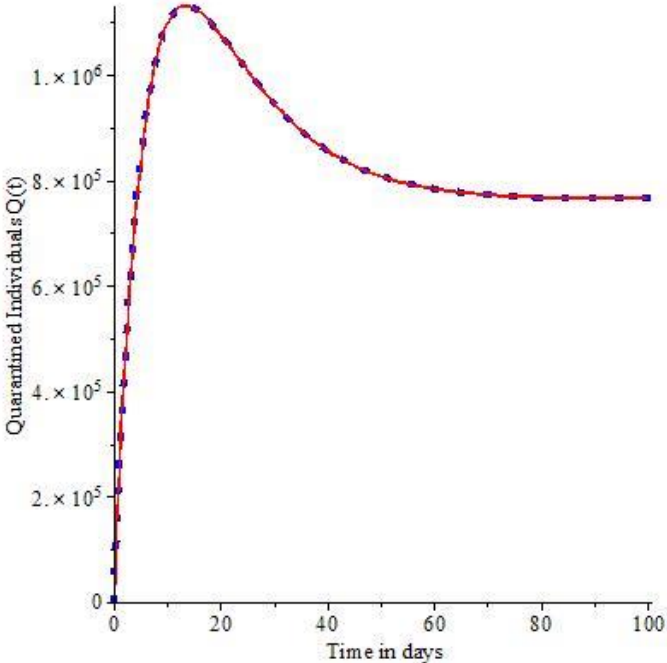


Figure 2: FABM and RK4 for $Q(t)$

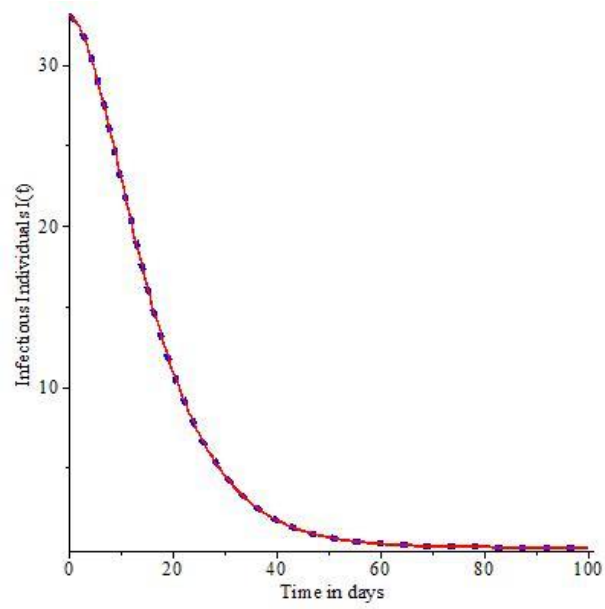


Figure 3: Comparison of FABM and RK4 for $I(t)$

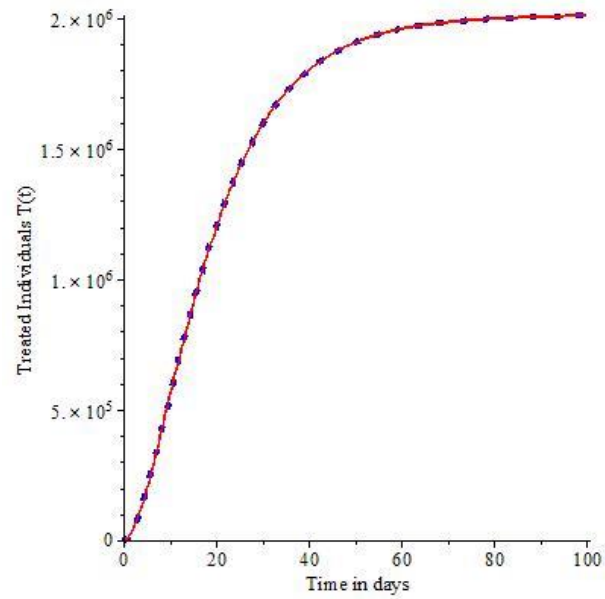


Figure 4: Comparison of FABM and RK4 for $T(t)$

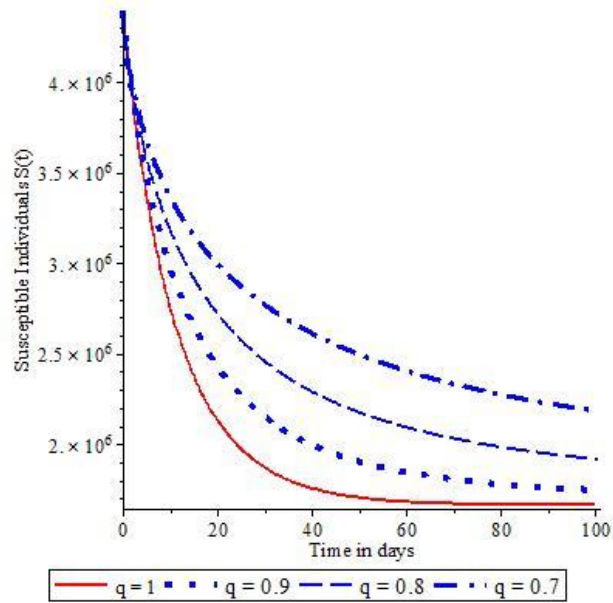


Figure 5: Effect of varying q on $S(t)$

The influence of memory index on the population of susceptible individuals is shown by Figure 5 for 100 days. Figure 5 shows that as the memory effect increases (that is, reduction in the value of q), the susceptible population increases.

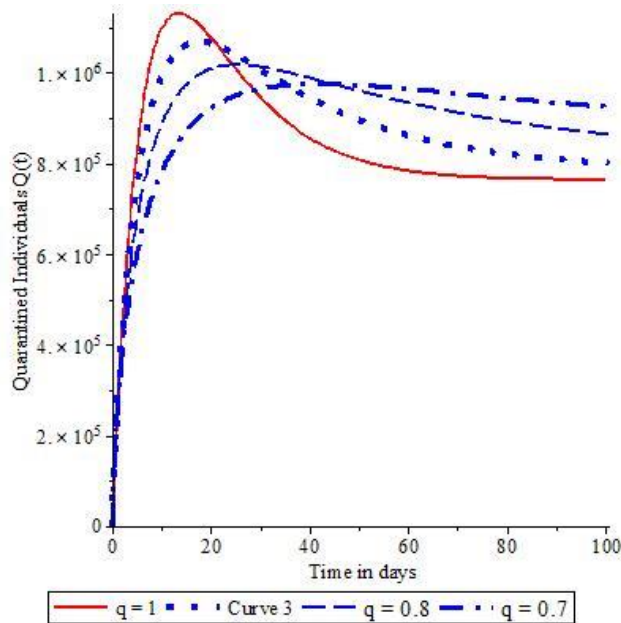


Figure 6: Effect of varying q on $Q(t)$

The effect of varying q on the quarantined population is displayed by Figure 6. There is a rapid increase in the population of the quarantined humans as q increases for about 25-30 days, before a sudden decrease.

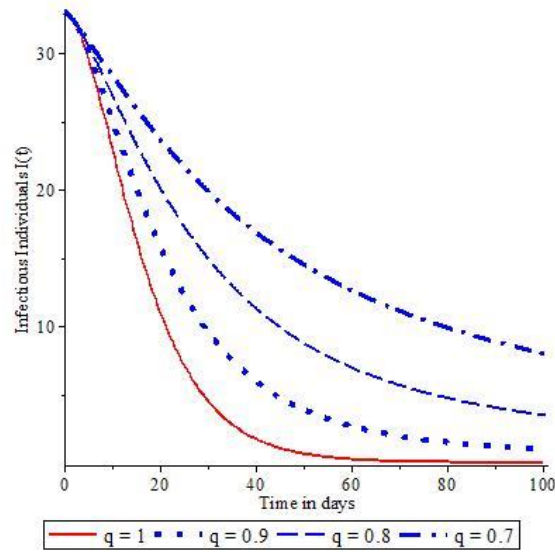


Figure 7: Effect of varying q on $I(t)$

The population profile for the infectious humans is shown by Figure 7 when the value of q is varied. Figure 7 displays that the population of infectious individuals increases as q reduces.

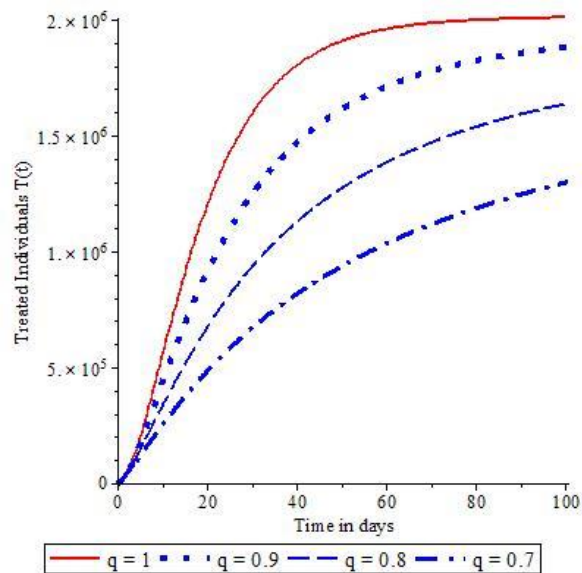


Figure 8: Effect of varying q on $T(t)$

The effect of varying q on the number of treated individuals is shown by Figure 8. Unlike the trend observed in Figures 5-7, the population of treated individuals decreases as q decreases.

Figures 5-8 therefore show the influence of memory index in the transmission dynamics of EVD as small changes in the memory index q result in big changes in susceptible, quarantined, infectious and treated populations respectively.

6 CONCLUSION

A fractional order model for EVD in the existence of contact tracing and isolation was formulated and solved numerically using the Fractional Adams Bashforth Moulton method. The results obtained from FABM method was compared graphically with those of fourth order Runge-Kutta method in order to validate its accuracy for integer case (that is for $q = 1$). The model is shown to be sensitive to q as small changes in q greatly influence the number of individuals in each subpopulation. The proposed method can be applied to solve other real life problems with memory effect.

REFERENCES

- [1] D. Catagna and G. Grassi, "Fractional-order systems without equilibria: The first example of hyperchaos and its application to synchronization," *Chinese Physics B*, vol. 24, no. 8, pp. 1-9, 2015.
- [2] S. Yang, A. Xiao, and H. Su, "Convergence of the variational iteration method for solving multi-order fractional differential equations," *Computers and Mathematics with Applications*, vol. 60, no. 10, pp. 2871-2879, 2010.
- [3] Y. I. Seo, A. Zeb, G. Zaman, and I. H. Jung, "Square-root dynamics of a SIR-Model in fractional order," *Applied Mathematics*, vol. 3, pp. 1882-1887, 2012.
- [4] M. Javidi and B. Ahmad, "A study of a fractional order cholera model," *Applied Mathematics and Information Sciences*, vol. 8, no. 5, pp. 2195-2206, 2014.
- [5] S. U. Haq, M. A. Khan, and N. A. Shah, "Analysis of magnetohydrodynamic flow of a fractional viscous fluid through a porous medium," *Chinese Journal of Physics*, vol. 56, no. 1, pp. 261-269, 2018.
- [6] R. Jan and A. Jan, "MSGDTM for solution of fractional order dengue fever," *International Journal of Science and Research*, vol. 6, no. 3, pp. 1140-1144, 2017.
- [7] M. Javidi and N. Nyamoradi, "Numerical Behaviour of a Fractional Order HIV/AIDS Epidemic Model," *World Journal of Modelling and Simulation*, vol. 9, no. 2, pp. 139-149, 2013.
- [8] A. Zeb, M. Khan, G. Zaman, S. Momani, and V. S. Erturk, "Comparison of numerical methods for SEIR epidemic model of fractional order," *Z. Naturforsch*, vol. 69, no. 1-2, pp. 81-89, 2017.

- [9] V. P. Latha, F. A. Rihan, and R. Rakkiyappan, "A fractional-order delay differential model for Ebola infection and CD8+T-cell response: Stability analysis and hopf bifurcation," *International Journal of Biomathematics*, vol. 10, no. 8, pp. 1-22, 2017.
- [10] I. Area, H. Batar, J. Losada, J. J. Nieto, W. Shammakh, and A. Torres, "On a fractional order Ebola epidemic model," *Advances in Difference Equations*, vol. 2015, no. 1, pp. 1-12, 2015.
- [11] A. Atangana and E. F. D. Goufo, "On the mathematical analysis of Ebola Hemorrhagic fever: deathly infection disease in West African countries," *BioMed Research International*, vol. 2014, Article ID 261383, 7 pages, 2014. <http://dx.doi.org/10.1155/2014/261383>.
- [12] Z. M. Odibat and S. Momani, "An algorithm for the numerical solution of differential equations of fractional order," *Journal of Applied Mathematics and Informatics*, vol. 26, no. 1, pp. 15-27, 2008.
- [13] S. O. Akindeinde, E. Okyere, A. O. Adewumi, O. O. Fabelurin, and S. E. Moore, "Caputo fractional order SEIRP Model for Covid-19 Pandemic," *Alexandria Engineering Journal*, vol. 61, pp. 829-845, 2022.
- [14] W. Ma, Y. Zhao, L. Guo, and Y. Q. Chen, "Qualitative and quantitative analysis of the COVID-19 pandemic by a two-side fractional-order compartmental model," *ISA Transactions*, vol. 124, pp. 144-156, 2022. <https://doi.org/10.1016/j.isatra.2022.01.008>.
- [15] A. Zeb, G. Zaman, V. S. Erturk, B. Alzalg, F. Yousafzai, and M. Khan, "Approximating a giving up smoking dynamics on adolescent nicotine dependence in fractional order," *PLOS ONE*, vol. 11, no. 4, pp. 1-10, 2016.
- [16] C. E. Madubueze, A. R. Kimbir, and T. Aboiyar, "Global stability of ebola virus disease model with contact tracing and quarantine," *Applications and Applied Mathematics*, vol. 13, no. 1, pp. 382 – 403, 2018.
- [17] P. A. Naik, "Global dynamics of a fractional-order SIR epidemic model with memory," *International Journal of Biomathematics*, vol. 13, no.8, 2050071, 2020.